



## Experiment Report Form

**The double page inside this form is to be filled in by all users or groups of users who have had access to beam time for measurements at the ESRF.**

Once completed, the report should be submitted electronically to the User Office using the **Electronic Report Submission Application**:

*<http://193.49.43.2:8080/smis/servlet/UserUtils?start>*

### ***Reports supporting requests for additional beam time***

Reports can now be submitted independently of new proposals – it is necessary simply to indicate the number of the report(s) supporting a new proposal on the proposal form.

The Review Committees reserve the right to reject new proposals from groups who have not reported on the use of beam time allocated previously.

### ***Reports on experiments relating to long term projects***

Proposers awarded beam time for a long term project are required to submit an interim report at the end of each year, irrespective of the number of shifts of beam time they have used.

### ***Published papers***

All users must give proper credit to ESRF staff members and proper mention to ESRF facilities which were essential for the results described in any ensuing publication. Further, they are obliged to send to the Joint ESRF/ ILL library the complete reference and the abstract of all papers appearing in print, and resulting from the use of the ESRF.

Should you wish to make more general comments on the experiment, please note them on the User Evaluation Form, and send both the Report and the Evaluation Form to the User Office.

### **Deadlines for submission of Experimental Reports**

- 1st March for experiments carried out up until June of the previous year;
- 1st September for experiments carried out up until January of the same year.

### **Instructions for preparing your Report**

- fill in a separate form for each project or series of measurements.
- type your report, in English.
- include the reference number of the proposal to which the report refers.
- make sure that the text, tables and figures fit into the space available.
- if your work is published or is in press, you may prefer to paste in the abstract, and add full reference details. If the abstract is in a language other than English, please include an English translation.



	<b>Experiment title:</b> <b>Micro-geometrical aspects of hydro-chemical degradation of natural and artificial fractured porous materials</b>	<b>Experiment number:</b> ME-37
<b>Beamline:</b> ID 19	<b>Date of experiment:</b> <b>from:</b> 07-02-01 7:00 <b>to :</b> 09-02-01 7:00	<b>Date of report:</b> August 30, 2002
<b>Shifts:</b> 6	<b>Local contact(s):</b> Elodie Boller	<i>Received at ESRF:</i>
<b>Names and affiliations of applicants (* indicates experimentalists):</b> <b>BERNARD Dominique</b> , ICMCB-CNRS, F-33608 PESSAC cedex <b>GOUZE Philippe</b> , UMR 5569, Univ. Montpellier II, F-34095 MONTPELLIER Cedex 5 <b>HEINTZ Jean Marc</b> , ICMCB-CNRS, F-33608 PESSAC cedex <b>VIGNOLES Gérard</b> , LCTS, F-33608 PESSAC cedex		

## Report:

In October 1999, our proposal ME-37 received less than half of the shifts we asked for (6 instead of 15). The main reason was the limited time available on ID19 before the important modifications that took place on this beamline. We decided to focus on one of the two aspects considered in the proposal (Hydro-chemical dissolution of micro-fractured carbonate rocks) and combining our time with the time allocated to ME-32, we have been able to perform preliminary experiments in October 2000 and in situ diagenetic evolution of carbonate rocks in February 2001. Experiments on artificial media (concrete, mortar) were performed on a complementary time allocation ME 285. Report on the experiments on artificial media (concrete, mortar) is then provided separately.

## Introduction

Carbonated rich rocks constitute a major reserve of fresh water throughout the world. Fractures, which develop in those relatively impermeable rocks, are the principal path for water but also for potential contamination. Fracture aperture may change strongly and quickly due to geochemical interactions between the fluid and the carbonate phase, leading to complex flow pathways. Presently, numerical models (ex: Dijk and Berkowitz, [1998, 2002]) do not take into account but the evolution of the fracture roughness and specific surface changes are although they theoretically play an important role in the control of the fluid-rock transfer rates at the initial stage of preferential dissolution, principally due to the lack of knowledge of the parameters that control dissolution processes: very few efforts have been done to understand, from experiments, the reciprocal effects of dissolution/precipitation processes on fracture characteristics, albeit indirect estimation of aperture changes through the measurement of hydraulic transmissivity is commonly performed. Experimental constraints are obviously required as these changes are complexly controlled by local geometrical and chemical properties which may produce gradually a large diversity of evolution rate of the individual fractures. The loss or gain of solute reactants  $\partial c_i / \partial t$ , corresponding to dissolution or precipitation of the rock forming minerals  $r_i$ , is controlled by thermodynamic parameters such as the

nondimensional saturation index and the kinetic mass transfer rate, but also to the extent of the contact  $S_s$  area between the fluid and the rock and its reactive portion,  $S_R$ , the reactive area.  $S_R$  is generally evaluated using geometrical models or from BET surface areas knowing the volume fraction of mineral  $r$ . For fractured tough rocks, BET method fails to individualize fracture wall specific surface. Alternatively, reactive surface area and the kinetic mass transfer can be evaluated from (1) measuring the difference in reactant concentration between the outlet and the inlet [Kieffer et al., 1999]. However, in the case of carbonate dissolution, continuous measurement of low concentration of reactants (ex: calcium) with specific probe is hopeless. Furthermore, this method still requires other information to access to  $S_s$  and  $S_R$  changes because it is a function of space and time as dissolution progresses.

Geometrical reconstruction seems to be much more realistic as far as it is possible to image the structure at a pertinent resolution. Comparing to other non-invasive method such as nuclear magnetic resonance imaging [Dijk et al., 1999; Brown et al. 1998], X-ray tomography is the only one that permits both pertinent field of view and accuracy as it was demonstrated by the ME 37 experiments.

### Experimental setup

Two samples of cretaceous limestone cored from the same borehole at few meters depth difference are studied. The first one, S1, is composed of 100 % (clay <1 w%) and a matrix porosity of 2.2 %. The second, S2, is composed of 85 w% calcite, 10 w% dolomite, 5 w% clay (silica <1 w%) and have a matrix porosity of 5.6 %. In both cases clay fraction is composed of about 50 w% of kaolinite, 5 w% of illite and 45 w% of interstratified smectite/illite (from X-ray diffractometry). For both the samples, a mini-core of 6mm diameter and 12mm long was prepared to suit the optimal object size of the European Synchrotron Radiation Facility (ESRF) ID19-X-ray beam for non-local computed micro-tomography (CMT). A tensile fracture, sub-collinear to the core axe, was made in each of the mini-core monoliths, and then mini-cores were epoxy coated to avoid any mechanical deformation during the percolation experiment.

We use the 2048 x 2048 pixels Fast REadout LOW Noise (FRELON) camera [Labiche 1996], equipped with an optical system leading to an effective pixel sizes of 4.91  $\mu\text{m}$ . This setup, using 120KeV photon beam, allows us to obtain a very intense, homogeneous, parallel and monochromatic X-ray beam of 10mm<sup>2</sup>. Finally tri-dimensional X-ray absorption image is computed [Johns et al., 1993; Herman, 1980] from the 900 radiographies acquired at every 0.2 degree of view angle. A bimodal segmentation algorithms based on challenge region growing was developed to extract the inlet-outlet-connected porosity (the fracture volume) from the solid phase. CMT resources was used to measure the change of the aperture and fracture surfaces geometry at different stage of dissolution during fluid flow of pure water enriched with carbon dioxide at partial pressure of 0.1 MPa. This solution (pH = 3.91 $\pm$ 0.05) is strongly under-saturated with respect to carbonate minerals and dissolution of the fracture surfaces takes place under control of kinetic processes. The pressure at the outlet was maintained higher than 0.1 MPa in order to avoid CO<sub>2</sub> degassing in the mini-core. Simplified diagrams of the mini-core imaging and flooding apparatus are illustrated in figure 1.

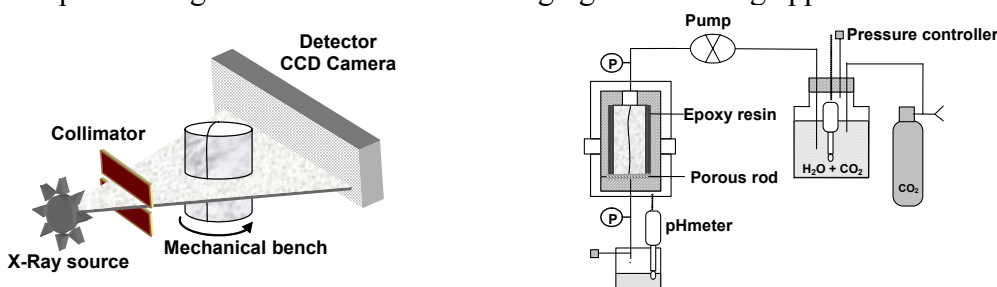


Figure 1 : Simplified diagrams of the mini-core imaging and flooding apparatus

### Results

The analysis of the fracture wall geometry is widely used for assessing several parameters that characterise the flow and the dispersion regimes [Adler and Thovert, 1999]. For example, one may calculate the change in the hydraulic section, mechanical aperture (to be compared to hydraulic aperture), the roughness and the correlation length of the surface topography (ex: fractality). A large number of publications discusses each of these aspects (for example Detwiler et al. [1999]) from observations based on mechanical or optical profilometry techniques. However this implies that fracture wall can be described as a 2D surface; but it will be established below that it is not always the case. On the first stage, we focussed on the determination of the fluid-rock interface characteristics and on their effects on the geochemical transfers in relation with the

fracture aperture changes. For a given mineral, dissolution can be characterised by the local Damkohler dimensionless parameter:

$$Da = \frac{S_R k <a>^2}{D_m} \quad (1)$$

where  $k$  is the kinetic reaction rate (1/time unit) far from equilibrium which is defined, for a given reaction, from time change of the concentration  $c$  of a the reactant,  $\partial c/\partial t = S_R k(1-c/c^*)$ , with  $c^*$  the corresponding at-equilibrium concentration. For small variation of the fluid composition,  $k$  can be assumed to be a constant. In (1)  $S_R$  is the non-dimensional reaction surface coefficient ( $S_R \geq 1$ ) At the initial stage, before dissolution,  $S_R$  can be practically estimated as the product of the volume fraction of the mineral involved in the given reaction, by the specific surface coefficient  $S_S$  which denotes the tortuosity of the fracture walls ( $S_S \geq 1$ ,  $S_S = 1$  for a planar surface). It is assumed that the fracture intersect the rock randomly, both in terms of mineral composition and of mineral size. Usually, for numerical modelling,  $S_R$  is kept constant and  $S_S$  is evaluated from the volume fraction of the mineral and embedded in an ‘efficient’ kinetic reaction rate [Lasaga, 1998]. The validity of this relation in the course of dissolution is questionable: ME 37 experiment results show that the relation between  $S_R$  and  $S_S$  is probably non-linear due to preferential dissolution in the case of the non-pure calcite S2. Fracture surfaces are analysed first of all using CMT projected image of the fracture wall which is directly analogous with what can be obtained using profilometer techniques. Initial and final (after dissolution) digital projected image of the fracture wall of S1 and S2 as well as cross sections are presented on figure 2. In addition, true tri-dimensional analysis of the fluid-rock interface was performed using the CMT volumic images.

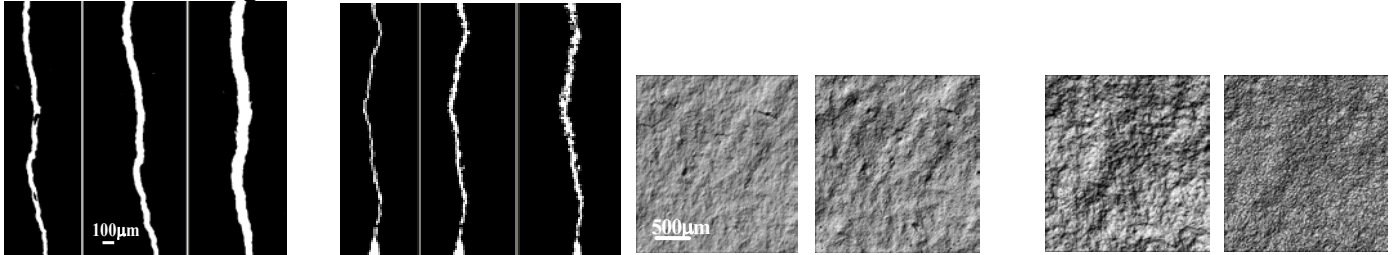


Figure 2: Initial and final (after dissolution) digital projected image of the fracture wall of S1 and S2 respectively (on the left) as well as cross sections (on the right)

The initial stage: For both samples, the initial fracture surfaces display an ubiquitous self-affine fractal behaviour at all measured scales (4 decades starting from  $\sim 5\mu\text{m}$ ). The fractal dimension, computed coherently using 1D and 2D power spectrum method (see for example Schmittbuhl et al. [1995 ]) is  $2.5 \pm 0.1$ , which denotes a random distribution of the surface topography. This value was confirmed using optical profilometer with a beam of  $30\mu\text{m}$  and a vertical accuracy of  $1\mu\text{m}$ . The area of self-affine fractal surface depends both on its fractal dimension and on  $\sigma^2$  the topography variance

The initial mean aperture along the central flow axe is  $45\mu\text{m}$  (rms=6) for S1 and  $20\mu\text{m}$  (rms=4) for S2.

Evolution of S1: The experiment comprises three dissolution steps with a mean aperture increase of  $22 \pm 2\mu\text{m}$  for each of them.

Dissolution of S1 is clearly a process of homogeneous chemical erosion of the surfaces. The fractal dimension of the surface topography calculated from the CMT remains constant at  $2.5 \pm 0.1$ . This value was verified on 20 profiles of 10 000 to 75000 data points of the final stage of the experiment using mechanical profilometer with a spike of  $2\mu\text{m}$  and a vertical accuracy of  $0.1\mu\text{m}$ . The invariance of the surface scale autocorrelation was also observed using the 3D-box-counting method (figure 3).

Evolution of S2: The experiment dissolution of S2 sample consists of three steps. Time duration for each of them was not constant resulting in a mean aperture increase of 4.5, 23 and  $15\mu\text{m}$  respectively. In contrast with S1, dissolution of S2 is noticeably heterogeneous. From the cross section of the final stage of the experiment (figure 2) one can observe that fracture walls cannot be described as a two-dimensional object. The analyses of 2D-projected digital image (equivalent to profilometer data) of the fracture walls give biased information on the structure changes as dissolution increases. Reliable information is given by the 3D-box-counting method. Figure n shows a slight increase of the fractal dimension as aperture growth denoting an increase of the surface autocorrelation for smaller scale. An essential characteristic of the S2 dissolution process is that aperture rms (measured along the central flow axe) increases by a factor 4 between the initial

and the final stage while aperture rms stay constant in the case of S1. This increase of the aperture distribution scattering denotes the increasing localisation of the dissolution at the sample scale.

Specific surface coefficient  $S_s(x,y)$  and fracture volume  $V(x,y)$  were measuring from the tri-dimensional images of S1 and S2. Correlation between SS and V were measured on a 250  $\mu\text{m}$  width stripe centred on the flow axe in order to avoid boundary effects (figure 4). Results show that the value of  $\langle S_s \rangle$  increase from 1.5 to 5, as it remains constant around 1.5 for S1. In the case of S1, a quasi-pure calcite rock, the reactive surface SR is therefore unchanged by the dissolution process. For S2, the linear increase of  $S_s$  measured in the experiment is significant although the non carbonate phase percentages are minor. However, this increase cannot persist indefinitely and the exploration of longer dissolution time is necessary to analyse appropriately the extension of this relation and the implication on the change in the reactive surface coefficient. Presently, it can be concluded from the V- $S_s$  apparently unconditional increasing relation, that the relation between SR and  $S_s$  is certainly non-linear because of the preferential dissolution of the carbonated phase.

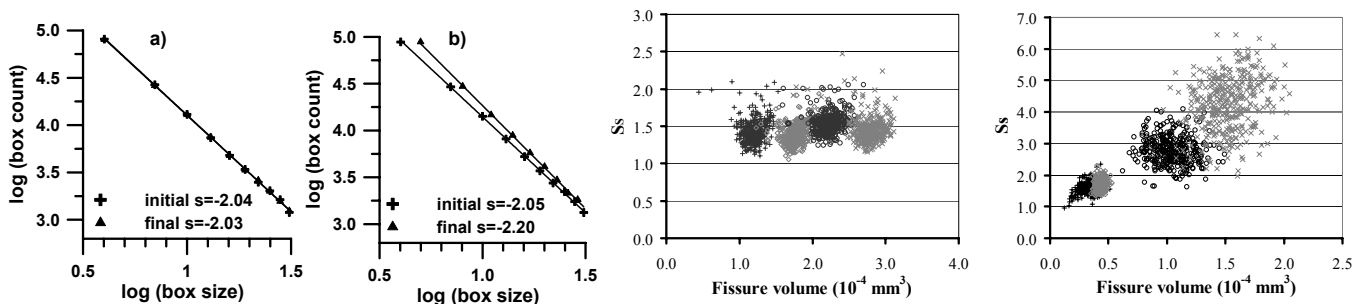


Figure 3 (left): Box counting diagram of the surfaces of S1 and S2 respectively

Figure 4 (right): Correlation diagram between fissure walls specific surface  $S_s$  versus fissure volume

For S1, one can note that the spreading of  $S_s$ -versus- $V$  data is unchanged from the beginning to the end of the experiment while the mean aperture increases of about 70  $\mu\text{m}$ . For this sample volume and aperture increases are linearly dependant as the fracture wall is intrinsically two-dimensional as demonstrated on figure 2. Oppositely, an increase of the data spreading in the V- $S_s$  domain with increasing dissolution is displayed on figure 3 for the sample S2. This scattering reflects the increasing dissolution localisation at the micro-scale observed on the cross sections (figure 2).

## Discussion and Conclusions

To our knowledge, there is very little similar published work. The most comparable one was proposed recently by Durham et al. [2001], although both the method and more importantly the mechanical aspect of the experiment differ strongly. For the method, the use of CMT instead of profilometry measurements is more convenient because it is not destructive and does not require opening out the sample to have access to the fracture surfaces. In their experiment, Durham et al. [2001] investigate the fracture properties changes of a marble submitted to a fixed confining pressure inducing a close up of the fracture while contact asperities are eroded. Conversely, the present work concerns the early stage of limestone dissolution at the subsurface where an increase of aperture and permeability is commonly observed. In the early stage of the fracture forming networks, fracture geometry and specific surface changes play an important role in the localisation of preferential flow path. The characterisation of archetypical modification arising as weathering start is essential for enriching and/or validating models such as those proposed recently by Dijk and Berkowitz [1998].

Experiments were conducted on two micritic rock sample. The first one is characteristic of the pure calcite end-member while the second, composed of 85 % of calcite, is characteristic of the average composition for marine carbonate environments. For both the sample, fracture surfaces keep self-affine fractal while aperture increases due to dissolution. Fractal dimension increases slightly for the non pure carbonate sample as it stays constant for the pure carbonate sample. For both the sample, aperture distribution evolves toward a complete Gaussian distribution (kurtosis and skewness equal 0), nevertheless the main measurable difference between the two samples is that the aperture rms increases strongly for the non-pure carbonate sample while it keeps constant for the pure carbonate sample. This increase of the aperture distribution scattering observed for the non-pure carbonate sample takes place together with the three-dimensional structuring of the fluid-

rock interface. The measurement of aperture rms is certainly the more pertinent parameter to identify the evolution toward complex three-dimensional fluid-rock interfaces if tomographic data are unavailable. For the quasi-pure calcite sample, the reactive surface coefficient which is, in this case, equal the specific surface coefficient remains constant throughout the dissolution process. Keeping in mind the maximum resolution wavelength ( $\lambda C = 4.91 \mu\text{m}$ ), the reactive surface is  $1.5 \pm 0.3$  times the projected surface area. However, this value is underestimated as the fracture surface is intrinsically self-affine fractal with a fractal dimension  $D = 2.5$ , and, by definition, the specific surface coefficient  $S_s$  is proportional to  $(\lambda C)^{D-2}$ . From SEM observations, one evaluates the average grain size at  $2 \mu\text{m}$  which implies that using  $\lambda C = 2 \mu\text{m}$ ,  $S_s$  is certainly close to 2.4.

Results, for the dissolution experiment of the non-pure calcite sample, allowed identifying the difficulties for quantifying the specific and reactive surface from the experimental characterisation of the fracture wall change in the course of dissolution. It is more specifically demonstrated here that the initial two-dimensional fluid-rock interface evolves rapidly toward a tri-dimensional interface which cannot be characterised from classical profilometry method. As a result of such an evolution, the total specific surface increases strongly in the first stage of the dissolution process. However, the SEM observations reveal that the calcite specific surface or reactive surface may not increase in the same proportion: the increase of the total specific surface is mostly due the increase of the exposed surface of the others mineral phases. S2 sample is typical of the worldwide marine carbonate environments and one may expect that the observed three-dimensional dissolution structure of the fracture wall is the regular evolution of such environments. The validity of the Hagen-Poiseuille “cubic law”:  $T(x,y) \sim g a(x,y) / 12 \nu$  (where  $g$  is the gravitational acceleration and  $\nu$  the kinematic viscosity), for natural fracture geometries have been discussed by many researchers, which broadly conclude that : i) The principal factor causing deviation from ideal parallel plate theory is the non-smooth geometry of fracture walls and ii) the aforementioned approximation is valid provided that an appropriate average aperture can be defined. Similar remarks stay, for example, for the determination of the dispersion coefficient (ex:  $D(x,y) \sim \langle u \rangle^2 a(x,y)^2 / 210 D_m$ ) from averaged or distributed aperture data. The occurrence of three-dimensional fluid-rock interfaces add difficulty to the discussion while unified definition the fracture aperture needed in the cubic law is not obtained when fracture walls are 2D structures. As important, dead-end three-dimensional voids that appear at the fracture walls are probably participating to the storage of solute, increasing the retardation factor for tracers and pollutants transport. Moreover, we assumed throughout the discussion that mechanical erosion is negligible, which was verified by the absence of particle in the outlet fluid. However, it is obvious that the structural evolution described for the sample S2 is strongly favourable to the loading of the fluid with undissolved minerals particles such as clays and silica. These particles and colloids are potential factors for tracers and pollutants retention and fracture clogging.

#### **REFERENCES:**

- Adler P.M. and Thovert J.F., Fractures and fractures networks, *Kluwer Academic Publishers*, 429p., 1999.
- Brown S., Caprihan A. and Hardy R., Experimental observation of fluid flow channels in a single fracture, *Journal of Geophysical Research* 103, B3, pp. 5125-5132, 1998.
- Detwiler R. L. and Rajaram H., Solute transport in variable-aperture fractures: An investigation of the relative importance of Taylor dispersion and macrodispersion, *Water Resources Research*, vol. 36, n°7, pp.1611-1625, 2000.
- Dijk P. and Berkowitz B. Precipitation and dissolution of reactive solutes in fractures, *Water Resource Research* 34, n°3, pp.457-470, 1998.
- Dijk P. and Berkowitz B., Measurement and analysis of dissolution patterns in rock fractures, *Water Resource Research* 38, n°2, pp.5-15-11, 2002.
- Dijk P., Berkowitz B and P. Bendel. Investigation of flow in water-saturated rock using nuclear magnetic resonance imaging (NMRI), *Water Resource Research* 35, n°2, pp.347-460, 1999.
- Durham W. B., Bourcier W. L. et Burton A., Direct observation of reactive flow in a single fracture. *Water Resources Research* 37, pp 1-12, 2001.
- Herman G.T., Image reconstruction from projections, Academic Press, New York, 1980.
- Johns R.A., Steude J.S., Castanier L.M, Roberts and Paul V., Nondestructive measurements of fracture aperture in crystalline rock cores using X ray computed tomography, *Journal of Geophysical Research*, vol. B98, no.2, pp.1889-1900, 1993.
- Kieffer B., Jové C., Oelkers E. and Schott J. An experimental study of reactive surface area of Fontainebleau sandstone as a function of porosity, permeability and fluid flow rate, *Geochim. et Cosmochim. Acta*, 63(21), P. 3525-3534, 1999.
- Lasaga A., Kinetic theory in the Earth sciences, monograph. *Princeton University Press, Princeton, NJ, United States (USA)*, 811 pp., 1998
- Schmittbuhl J and Vilotte J.P., Reliability of self-affine measurements, *Physical Review E* 51, pp.131-147, 1995.